Review Comments

In total, we received feedback from two reviewers. The history of the detailed discussion we had between these two reviewers is provided below.

Reviewer #1: This paper presents a data-driven framework for modeling nonlinear sloshing dynamics. The proposed scheme is based on gradient-based embedding, spectral decomposition, and sequential sparse regression. The average mutual information and false nearest neighbors method were considered to select the delay step and embedding dimension in phase space reconstruction. The embedded sloshing sequence is subsequently decomposed into two parts: linear evolution and nonlinear excitation. A predictive model is developed using the decomposed components. The method proposed is innovative and the scientific quality of this manuscript is generally satisfactory. In this sense, this manuscript brings substantial new contributions. Based on that, I do recommend the acceptance of this manuscript after the following aspects are improved.

Reviewer #3: This paper analyzes the sloshing phenomenon in the ML-based framework. The advantage of ML is that simulation can be reproduced without utilizing any governing equations. This paper has shown the potential of the ML-based method for solving the sloshing problem. The authors demonstrated their numerical methods for characterizing the sloshing phenomenon in a tank with slat screens. The topic is of interest and the problem is worthy of study. The paper is well written. The following comments should be addressed before the recommendation of the paper for publication in ”Ocean Engineering”.

First Round Discussion

- Participant
  - Atilla Incecik
  - Reviewer #1
  - Reviewer #3
  - Xihaier Luo
  - Ahsan Kareem
  - Liting Yu
  - Shinjae Yoo
- Time: January, 9, 2022 - March, 17, 2022

To Reviewer #1

We appreciate the valuable insights from the reviewer. In the following we offer our point-by-point responses to each of the comments.

To Comment #1

Concern: ***In Section 3, the authors should give a detailed description of the experimental results, which will be used for data-driven modeling.***

Response: Thank you for the reviewer's advice. We added more details to the Section 3.1 and a graph showing the test tank, screen placement, and screen parameters. In addition, we set up a GitHub repository and uploaded a detailed description of the experiments we conducted in order to better communicate with the reviewer and future readers. In particular, it contains the specific screens parameters and excitation frequency tested for all 539 experiments.

Revised Section 3

The experimental data for this work was provided by the Laboratory of Vibration Test and Liquid Sloshing at Hohai University in China [1, 2]. A six-degree-of-freedom motion simulation platform, also known as a hexapod, was used in particular to generate the liquid tank's motions based on a specified input of time histories. A rectangular plexiglass tank with internal dimensions of $1000\,mm \times 700\,mm \times 100\,mm$ (length $\times$ height $\times$ width) is employed. It is $8mm$ thick and partially filled with water, with the liquid depth-to-tank-length ratio set at 0.12. Vertical slat screens made of perforated steel plates are used to prevent shallow water sloshing. Furthermore, a horizontal sinusoidal motion defined by $X(t) = A\sin(\omega t)$ is applied to the platform. Note $A/l = 0.01$ with l denoting the length of the tank. A wide range of frequencies have been tested. The range of the motion frequency is 1.70 rad/s- 17.71 rad/s (0.27 Hz - 2.5 Hz). The specific screens parameters (number (represented by m), solidity ratio(represented by Sn), slot diameter (represented by Zp (mm)), d/a) (See Fig. 1) and excitation frequency (f (Hz)) tested is listed in the supplementary material, which

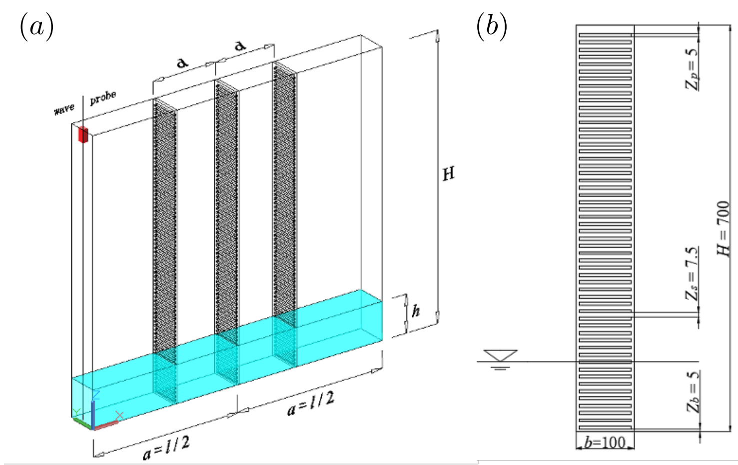

Figure 1: (a) The test tank and the position of screens, (b) example of screens parameters (unit: mm).

is publicly available at `https://github.com/Xihaier/ML_Sloshing_Characterization` The displacement of the motion platform was recorded by a displacement sensor. A wave probe (WH200) located at a distance of 15 mm from the left vertical wall is used to track the evolution of the free-surface elevations near the tank wall. As a result, a total of 539 sequences, where each sequence corresponds to a specific experiment configuration, have been recorded for analysis. A more detailed experimental setup is available in [1, 2].

To Comment #2

Concern: ***Fig.6 is not found in the manuscript.***

Response: Thank you for alerting us to this issue. We double-checked the revised manuscript in various PDF readers to ensure that it was properly inserted. We also uploaded the metadata, as well as each figure, to the system. Please let us know if you continue to have trouble accessing the figure. We can get in touch with the journal coordinator or editor to directly share the figure with you.

To Comment #3

Concern: ***In section 3.4, it is difficult to distinguish chaotic motion of free surface from the trajectories plotted in the reconstructed phase space. In fact, according to the external excitation frequency and the geometry of the cavity, the liquid free surface may produce very complex nonlinearities such as out-of-plane sloshing, spinning, irregular beat vibration, pseudo-periodic motion and chaos, these nonlinearities are much more complex than the "elevation first runs up and then runs down" that the authors point out.***

Response: Yes, we agree with the reviewer's observations about the nonlinear properties of water sloshing. We are working on wave numerical simulation in a 2D/3D tank and intend to upgrade our current experimental platform. We are validating the numerical model for simulation using experimental results [1]. For experiments, we intend to install more sensitive sensors to better monitor the water waves [2]. We have revised our conclusion about the future endeavor accordingly.

- 1. This folder contains our current work on simulating violent sloshing flows (`https://github.com/Xihaier/ML_Sloshing_Characterization`). We intend to devote more resources to improving the accuracy and robustness of our current implementations. We will conduct the characterization analysis proposed in this manuscript after the model has been adequately validated to provide a more comprehensive study of the nonlinear dynamics.

- 2. Kim, S.Y., Kim, K.H. and Kim, Y., 2015. Comparative study on pressure sensors for sloshing experiment. Ocean Engineering, 94, pp.199-212.

Revised Conclusion

This paper proposes a framework for characterizing the dynamics of nonlinear and non-Gaussian liquid sloshing. In comparison to traditional system identification methods like wavelet, the proposed machine learning framework provides approximate linear representations of nonlinear dynamics. To address the data rank-deficiency, spectral decomposition is applied to time delay coordinates given a sequence of wave elevation. Then, using a set of decomposed eigenvectors, sequential sparse regression is utilized to identify an intermittently forced linear system. As a result, when compared to traditional approaches, the model's transparent data-driven structure and fast machine learning computation make it an excellent candidate for online feedback control tasks. In future work, it is worthwhile to incorporate well-established controlling strategies into the current framework.

Through the use of a wide range of experimental data, we demonstrated the model is capable of accurately representing embedded sloshing sequences. Meanwhile, a series of statistical tests show that the model captures chaotic behaviors like bursting and switching in the embedded sequence. Various performance metrics are used to demonstrate the accuracy of the multi-step prediction results. Admittedly, liquid sloshing can cause complex nonlinearities such as out-of-plane sloshing, spinning, irregular beat vibration, and pseudo-periodic motions. These nonlinearities are far more complex than the wave elevation dynamics we observed. Extending the methodology described here to different types of moving water waves, using either high fidelity CFD simulation data or more delicate experiment measurements, is a desirable first step toward developing a more robust and general data-driven simulation strategy for sloshing dynamics.

To Comment #4

Concern: ***The reviewer suggests the author give a brief review about the recent research on the large amplitude liquid sloshing and the published paper shown below should be included in the reference list: 1) Yong Tang, Baozeng Yue. Simulation of Large-Amplitude Three-Dimensional Liquid Sloshing in Spherical Tanks, AIAA Journal, Vol. 55, No. 6:1-8. 2017. 2) Yong Tang, Baozeng Yue, Yulong Yan. Improved method for implementing contact angle condition in simulation of liquid sloshing under microgravity. International Journal for Numerical Methods in Fluids, Vol. 89, No. 4-5: 10-20, 2019.***

Response: Thank you for sharing the important research on large amplitude liquid sloshing. We updated our introduction to include the work done in these two papers.

Revised Introduction

Partial differential equations (PDEs) are frequently used to describe the principles that govern physical systems in the modern world. These specified PDEs, also known as governing equations, aid in the establishment of scientific fields and the rapid advancement of technology. In the context of liquid sloshing, potential flow theory was used to simulate small-amplitude sloshing motion in a regular-configuration container [3, 4]. The Laplace equation was later used to analyze nonlinear sloshing problems in two/three dimensions for more turbulent scenarios. When solved using the finite element method or the boundary element method, the computed results can capture free surface sloshing motions in various liquid storage tanks [5, 6, 7]. Another possibility is to use Navier Stokes equations to solve the problem. To simulate viscous liquid sloshing in a baffled tank with possibly broken free surfaces, several turbulence models, including Reynolds averaged Navier–Stokes (RANS) and large-eddy simulation (LES), were evaluated [8, 9, 10]. However, when large amplitude sloshing occurs traditional finite element-based methods frequently fail to provide accurate results. To address this issue, advanced numerical methods such as arbitrary Lagrangian-Eulerian elements [11, 12] and smoothed particle hydrodynamics [13, 14] are introduced, where the former focuses on maintaining a high-quality mesh throughout an analysis when large deformation occurs and the latter is meshless and uses a collection of pseudo-particles to represent a given body.

While knowing these equations and using advanced numerical methods allow us to simulate liquid sloshing in a variety of tanks, reliable and high-fidelity PDE-governed models remain elusive in many tank and baffle settings.

To Reviewer #3

We appreciate the careful reviewing and in-depth observations made by the reviewer. The comments are very helpful and we have revised accordingly.

To Comment #1 & #9

Concern:

- ***Please explain the meaning of signal bursting and switching as it will be seen in the sloshing problem.***
- ***In Figure 7, does the convergence of the trajectory mean that the fluid responses reach the steady state in their time history? There are three types of shapes of the converged path of the attractor (saddle, circle, and hyper track). Could you relate it to some features such as sloshing motion or sloshing dynamic characteristics?***

Response: Physically, swirling wave motion, also known as rotary sloshing, is responsible for signal bursting and switching of interest. It is very common in liquid sloshing in a rectangular tank. When the forcing frequency is increased slightly more, the swirl wave abruptly collapses and the motion shifts to a small-amplitude out-of-phase planar wave motion [1,2]. Throughout some of the experiments, we observed the formation of bubbles, which eventually burst on the liquid's free surface. However, from the standpoint of machine learning, the input is wave elevation. Following [3], we hypothesize that the interaction of water and tank wall is analogous to a simple pendulum. A wave is reflected when it strikes a hard vertical surface. The wall pushes the water back just as

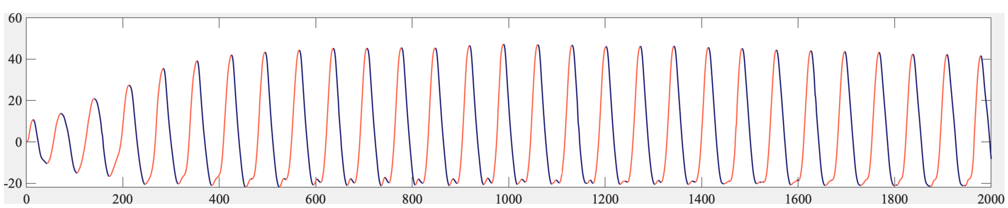

(a) Sloshing time series: state-space representation

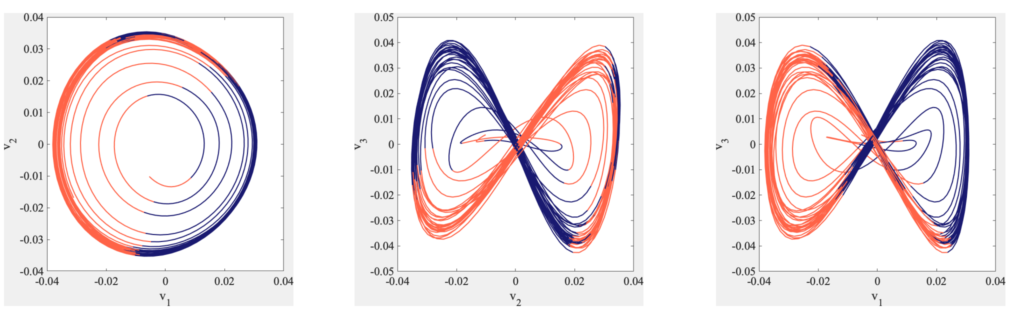

(b.1) Embedded eigen-space representation: (v_1, v_2)

(b.2) Embedded eigen-space representation: (v_2, v_3)

(b.3) Embedded eigen-space representation: (v_1, v_3)

Figure 2: Connection between state-space representation and eigen-space representation.

hard as it was pushed, causing waves to form in the opposite direction. As a result, the elevation changes. For this reason, we divide our signal into rising (orange in color) and falling (blue in color) intervals based on the elevation in the state space. The trajectory clearly moves along an attractor with two lobes (Fig. 2 (b.2) and (b.3)), switching back and forth between the two lobes intermittently by passing near a saddle point in the middle of the domain. We can see that the trajectory is not perfectly separated. Ideally, it should be half orange and half blue. This could be due to the fluids' inertia, which prevents them from quickly turning in the flow direction along the oscillation of the tank. That is why there is a time lag in eigen-space.

It is worth noting that we are linking the decomposed results of embedding elevation sequences to the observations. In addition to investigating the leading components, we performed additional tests on the decomposed components' forcing term in order to establish a proper physical interpretation. Fig. 3 depicts the probability density function of the forcing term. We used various types of density functions to fit the data. When compared to the normal distribution, the long tails captured by the nonparametric method indicate rare intermittent switching events. Long tails in probability density functions are well-known for studying dynamic rare events in climate and ocean waves [4,5]. We performed the same analysis on the other two clusters, and the computed results are available at `https://github.com/Xihaier/ML_Sloshing_Characterization`.

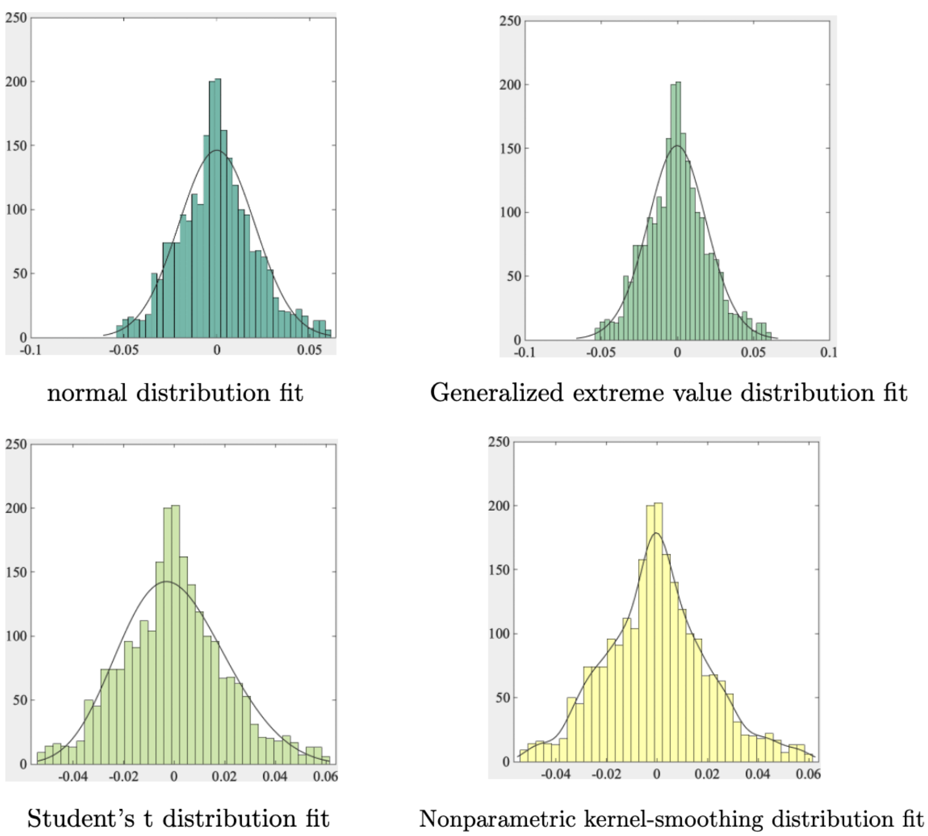

Figure 3: Probability density function of the forcing term.

However, the statistics of wave elevation alone may be insufficient to characterize the switching dynamics. To collect more data, we intend to run CFD simulations. Provided with sufficient data from a high-fidelity simulation model, the method can be applied to state-space data without embedding it in a higher dimension to expand the underlying dynamics. It would also be more convenient to define physically interpretable bursting and switching signals. At the present stage, we are developing and validating our CFD model. Some preliminary simulation results can be found at `https://github.com/Xihaier/ML_Sloshing_Characterization`.

Lastly, we would like to confirm the reviewer's observation on *the convergence of the trajectory indicate that the fluid responses reach the steady-state in their time history* is correct (See Fig. 4). To be more specific, we see a periodic pattern. Some experiments' amplitudes are decreasing, while others are nearly constant or increasing. We intend to conduct additional experiments with more sensitive sensors to confirm this finding in the future.

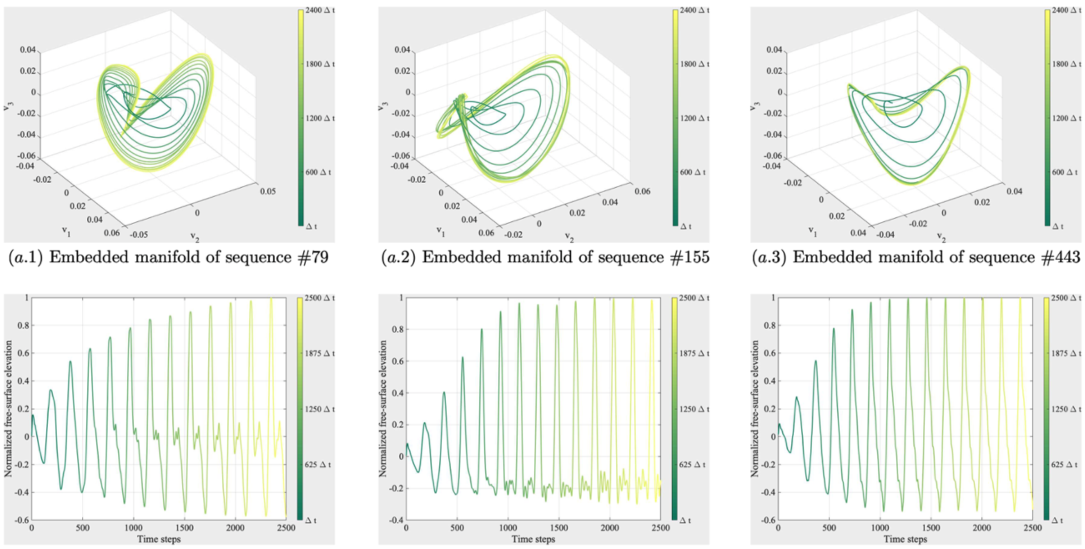

(a.1) Embedded manifold of sequence #79 (a.2) Embedded manifold of sequence #155 (a.3) Embedded manifold of sequence #443

(b.1) Time history of sequence #79 (b.2) Time history of sequence #155 (b.3) Time history of sequence #443

Figure 4: Time history of sloshing sequences and their embedded attractors.

- 1. Royon-Lebeaud, A., Hopfinger, E.J. and Cartellier, A., 2007. Liquid sloshing and wave breaking in circular and square-base cylindrical containers. Journal of Fluid Mechanics, 577, pp.467-494.
- 2. Carra, S., Amabili, M. and Garziera, R., 2013. Experimental study of large amplitude vibrations of a thin plate in contact with sloshing liquids. Journal of Fluids and Structures, 42, pp.88-111.
- 3. Ibrahim, R.A., 2020. Assessment of breaking waves and liquid sloshing impact. Nonlinear Dynamics, 100(3), pp.1837-1925.
- 4. Cousins, W. and Sapsis, T.P., 2014. Quantification and prediction of extreme events in a one-dimensional nonlinear dispersive wave model. Physica D: Nonlinear Phenomena, 280, pp.48-58.
- 5. Cousins, W. and Sapsis, T.P., 2016. Reduced-order precursors of rare events in unidirectional nonlinear water waves. Journal of Fluid Mechanics, 790, pp.368-388.

To Comment #2

Concern: ***Some paragraphs are unclear to me. On page 7 line 9, "the HAVOK model first factorizes aaa using spectral decomposition methods". On page 10 line 37, "vertical slat screens composed of perforated aaa steel plates." On page 12 line 9, "The maximum number of iterations for the k-means++ algorithm".***

Response: Yes, thank you for bringing this to our attention. We performed a systematic check for typos, grammatical errors, and spelling errors.

Revised lines

- To characterize the dynamics, the HAVOK model first factorizes $\boldsymbol{X}$ using spectral decomposition methods.
- Vertical slat screens made of perforated steel plates are used to prevent shallow water sloshing.
- The k-means++ algorithm, by definition, iteratively improves the quality of the solution by removing one cluster, dividing others, and re-clustering in each iteration. We set the maximum number of iterations to 1000 for fast evaluation, which means that iteration stops after this many iterations even if the convergence criterion is not satisfied.

To Comment #3 & #4

Concern:

- ***SVD is often used for linear systems, please explain the extension for the nonlinear data.***
- ***In your case, if X represents the wave elevation, then please explain the physical meaning of the U, Σ, V.***

Response: Thank you for bringing this up. To begin with, we agree with the reviewer that the analysis of the sloshing phenomenon appears difficult due to instabilities, nonlinearities, and turbulence. To address this issue, fluid mechanics community typically assumes that there are key underlying phenomena that serve as the foundation of many flows. Indeed, mounting evidence has shown that common flow features emerge across a wide range of fluid flows, such as von Kármán vortex shedding and the Kelvin–Helmholtz instability [1]. Following the same principle, SVD is used as a modal analysis technique in this work to extract the underlying flow features from experimental data.

From a mathematical perspective, modal analysis is carried out by applying decomposition algorithms to the collected data. Eigenvalue decomposition, in particular, assists us in identifying a linear subspace to describe the nonlinear field of interest. It can be used to investigate the iterative effects of the operator, such as $f(x) = x^k$ and $f(x) = \exp(xt) = I + xt + \frac{1}{2}x^2x^2 + \cdots$. The SVD algorithm is a matrix factorization algorithm that extends the eigendecomposition to rectangular matrices. The SVD, like the eigenvalue decomposition, can be interpreted as a way to represent the effect of matrix operation simply by multiplying by scalars in the appropriate directions. Because the SVD is applied to a rectangular matrix, two sets of basis vectors are required to span the matrix's domain and range. If $A = U\Sigma V^*$ ($*$ denotes the conjugate transpose), we have the right singular vectors V spanning the domain of A and the left singular vectors U spanning the range of A. This is not the same as the eigenvalue decomposition of a square matrix, where the domain and range are generally the same.

In terms of practical application, SVD serves as the foundation for many fluid analysis tools such as proper orthogonal decomposition (POD) and dynamic mode decomposition (DMD) [2, 3]. POD, for example, extracts modes by optimizing the mean square of the field variable under consideration. It decomposes a set of data into as few basis functions or modes as possible in order to capture as much kinetic energy as possible. It should be noted that due to the experimental constraints, we only have a scalar measurement. This is why we form the matrix A using time-delay embedding. The Takens embedding theorem, which provides a rigorous framework for analyzing the information content of measurements of a nonlinear dynamical system, is used as the basis for such analysis assumptions. Given this, U can be interpreted as a set of basis functions or modes of embedded wave elevation, and V as a set of time residuals solved by the optimization problem. The eigenvalue, which is stored in Σ, ranks the column vectors/modes of U. We admit that SVD arranges modes U in the order of their energy contents rather than their dynamical importance. It would be worthwhile to develop new decomposition algorithms, particularly those that allow for the incorporation of physical constraints in order to capture the dynamics of nonlinear systems with large transient growth from a non-engerigtic standpoint.

Throughout the paper, we present a machine learning method for identifying linear representations of nonlinear dynamics. To accomplish this, we used the Koopman operator. Take, for example, a dynamical system of the form

$$\frac{d}{dt}\mathbf{x}(t) = \mathbf{f}(\mathbf{x}(t)) \tag{1}$$

The starting point in our case is the discrete-time experimental data. As a result, we're looking for a discrete-time propagator that can $\mathbf{x}_{k+1} = \mathbf{F}\left(\mathbf{x}_k\right)$. The following is the relationship between continuous and discrete operators:

$$\mathbf{F}\left(\mathbf{x}_k\right) = \mathbf{x}_k + \int_{k\Delta t}^{(k+1)\Delta t} \mathbf{f}(\mathbf{x}(\tau))d\tau \tag{2}$$

Historically, the traditional geometric perspective of dynamical systems describes the topological organization of trajectories. In this paper, we propose Koopman analysis as an alternative method for describing the evolution operator that advances the space of measurement functions of the dynamical system's state. The Koopman operator, by definition, is an infinite-dimensional linear operator that advances measurement functions of the state forward in time in accordance with the dynamics in

$$\mathcal{K}g = g \circ \mathbf{F} \quad \Longrightarrow \quad \mathcal{K}g\left(\mathbf{x}_k\right) = g\left(\mathbf{x}_{k+1}\right) \tag{3}$$

The SVD is used to decompose the finite approximation of the infinite-dimensional Koopman operator that linearizes nonlinear dynamics. This is how we extend SVD to nonlinear data [4].

- 1. Taira K, Brunton SL, Dawson ST, Rowley CW, Colonius T, McKeon BJ, Schmidt OT, Gordeyev S, Theofilis V, Ukeiley LS. Modal analysis of fluid flows: An overview. Aiaa Journal. 2017 Dec;55(12):4013-41.

- 2. Lumley, J.L., 1967. The structure of inhomogeneous turbulent flows. Atmospheric turbulence and radio wave propagation.

- 3. Schmid, P.J., 2010. Dynamic mode decomposition of numerical and experimental data. Journal of fluid mechanics, 656, pp.5-28.
- 4. Luo, X. and Kareem, A., 2021. Dynamic Mode Decomposition of Random Pressure Fields over Bluff Bodies. Journal of Engineering Mechanics, 147(4), p.04021007.

To Comment #5

Concern: ***In your experiments, does breaking wave occur? How do you evaluate the wave elevation as wave breaks?***

Response: Thank you for the question. In experiments, there is the phenomenon of breaking waves. The test results show that the use of screens significantly reduces sloshing. As a result, in order to measure the sloshing wave height in the tank with screens, the excitation amplitude was increased to A/l=0.01(A=10mm). However, when the excitation amplitude is A/l=0.01(A=10mm) for the tank without screens, wave breaking occurs when the excitation frequency is close to the sloshing natural frequency. Given that the primary goal of this paper is to investigate the application of machine learning methods in the sloshing phenomenon, and that after installing screens, there are a large number of fine slots of screens, which greatly increases the time-consuming of numerical calculation, we attempt to replace the numerical method with machine learning methods. We admit we used a rough treatment method in the paper. We ignore the influence of wave breaking in the tank without screens when measuring sloshing wave height at large excitation amplitudes and resonant excitation frequencies. We plan to upgrade our current experimental equipments in the future and conduct a more systematic investigation of the breaking wave phenomenon.

To Comment #6

Concern: ***Please provide the resolution and sampling rate of the wave gauges.***

Response: Yes. The range and resolution of the wave probe are 40 cm and ± 0.5 % F·S, respectively. The time series of free surface elevation has been recorded and saved by the data acquisition system SDA1000 at a sampling rate of 100 Hz over 40 s.

To Comment #7 & #8

Concern:

- ***On page 13 line 22, "Third, the second cluster sequences have a higher excitation frequency, whereas the other two clusters have higher harmonic periods." looks weird since w1 ∈ [2, 3] while w2 ∈ [0, 1] and w3 ∈ [1, 2].***
- ***On page 13 line 25, "Despite the fact that cluster 2 and cluster 3 sequences have only one dominant frequency band, the bandwidth is strongly influenced by the external excitation frequency". I wonder the reason of how it relates to the external excitation frequency. Please try to correlate the bandwidth in the wavelet diagram with fluid kinetic energy.***

Response: Thank you so much for bringing this to our attention. We double-checked the experiment settings and updated the results accordingly. N_{S_n} denotes the number of slat screens, S_n is the solidity ratio, Z_p is the slot height, Z_b is the distance between the lowest slot and the slat screen bottom, A is the excitation amplitude, and ω is the excitation angular frequency. Note the slat screen dimensions are in mm. The hypothesis of the reviewer is correct. The wavelet analysis results show that the proposed clustering algorithm successfully clustered sloshing sequences with similar dynamics (similar excitation frequency).

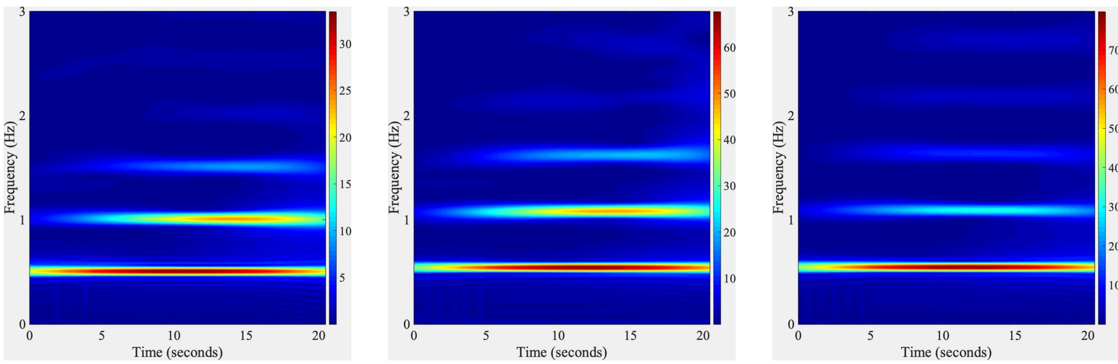

(a) sequence # 79 (b) sequence # 155 (c) sequence # 443

Figure 5: Wavelet analysis results of cluster 1 sequences.

Sequence	N_{S_n}	S_n	Z_p	Z_b	A	ω
# 79	1	0.6	5	0	10	0.5
# 155	1	0.4	50	0	10	0.53
# 443	2	0.6	5	0.8	10	0.54

Table 1: Experimental parameters of cluster 1 sequences.

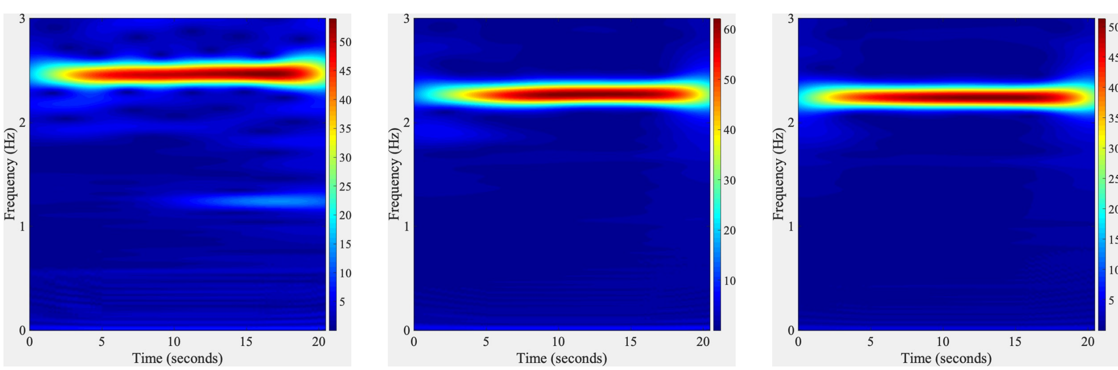

(a) sequence # 120 (b) sequence # 387 (c) sequence # 535

Figure 6: Wavelet analysis results of cluster 2 sequences.

Sequence	N_{S_n}	S_n	Z_p	Z_b	A	ω
# 120	1	0.6	5	0	10	2.45
# 387	2	0.6	5	0.5	10	2.25
# 535	3	0.6	5	0.5	10	2.22

Table 2: Experimental parameters of cluster 2 sequences.

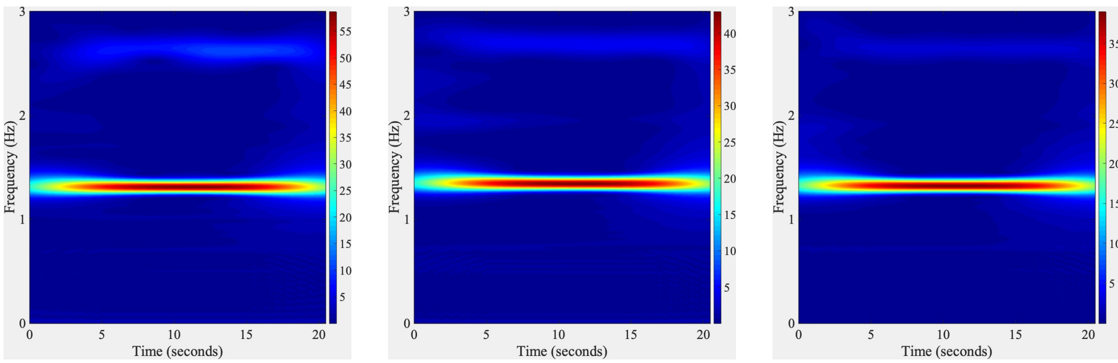

(a) sequence # 96 (b) sequence # 411 (c) sequence # 500

Figure 7: Wavelet analysis results of cluster 3 sequences.

Sequence	N_{S_n}	S_n	Z_p	Z_b	A	ω
# 96	1	0.6	5	0	10	1.3
# 411	2	0.6	5	0.66	10	1.33
# 500	3	0.6	5	0.5	10	1.31

Table 3: Experimental parameters of cluster 3 sequences.

To Comment #10

Concern: ***Figure 8 shows the similarity of the patterns from under-, optimally, and over-fitted results. Please explain the definition of optimally learned reconstructed results. A figure of training number vs accuracy or reconstructed length vs accuracy could be useful.***

Response: Thank you for bringing this to our attention. Figure 8 depicts an attractor reconstruction that is used to infer geometrical and topological information about the embedded sloshing sequence. The main goal here, from a modeling standpoint, is to find the best fit using the eigenbasis identified by SVD. Adapted from the concept from the machine learning community [1], under-fitted results are those produced by a model that is unable to capture the data geometry. This could be due to a lack of sufficient basis to describe the attractor's trajectory. Over-fitted results are those produced by a model that models the data geometry at some given points far too well. This could be due to the use of too many higher modes, which are notoriously noisy and fluctuating in practice. As a result, the results may be very curly. Ideally, we want to choose a model that falls somewhere between under-fitting and over-fitting. As a result, we looked at the reconstruction results with a different number of components. We've included the reconstruction results for a randomly chosen sequence from the other two clusters below in the hopes that they'll help the reviewer understand what we mean by under-, optimally-, and over-fitted results.

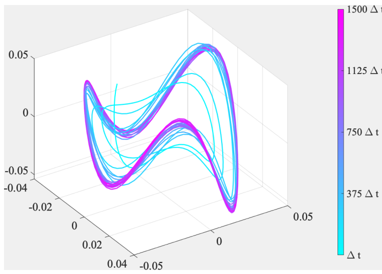

(a) ground truth

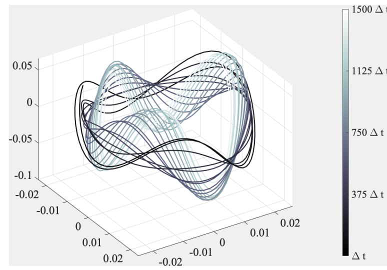

(b) underfitted results

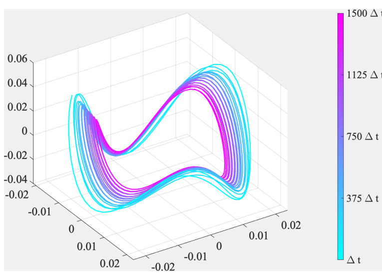

(c) optimally fitted results

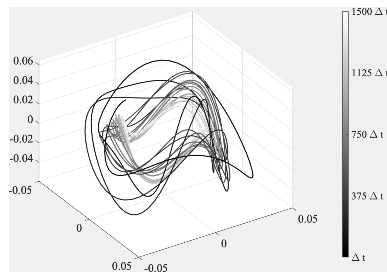

(d) overfitted results

Figure 8: Reconstructed embedded attractor results of the sequence #501.

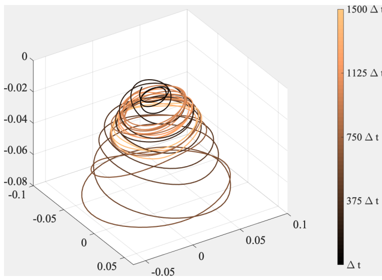

(a) ground truth

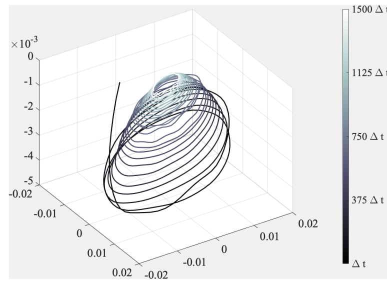

(b) underfitted results

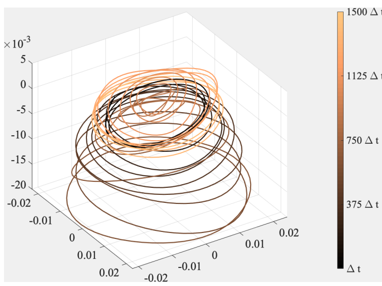

(c) optimally fitted results

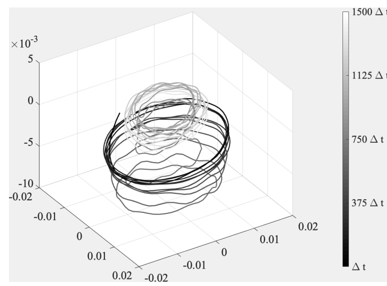

(d) overfitted results

Figure 9: Reconstructed embedded attractor results of the sequence #34.

Thank you very much for your excellent suggestion. We drew a graph to show the relationship between the number of components/basis and accuracy. It should be noted that we originally looked at the reconstruction results in terms of the number of basis functions. Finding a metric that is reliable across a large number of basis functions can be difficult because each model may identify a different eigenbasis from the SVD results. Simply averaging the error in each direction may be deceptive because some bases have little direct contribution to the fitting process. For this reason, we experimented with various methods and metrics before settling on two: (1) the leading component's normalized error, as measured by its contribution to the overall geometry; and (2) the leading component's normalized correlation. The lower the error, the better, and the higher the correlation, the better.

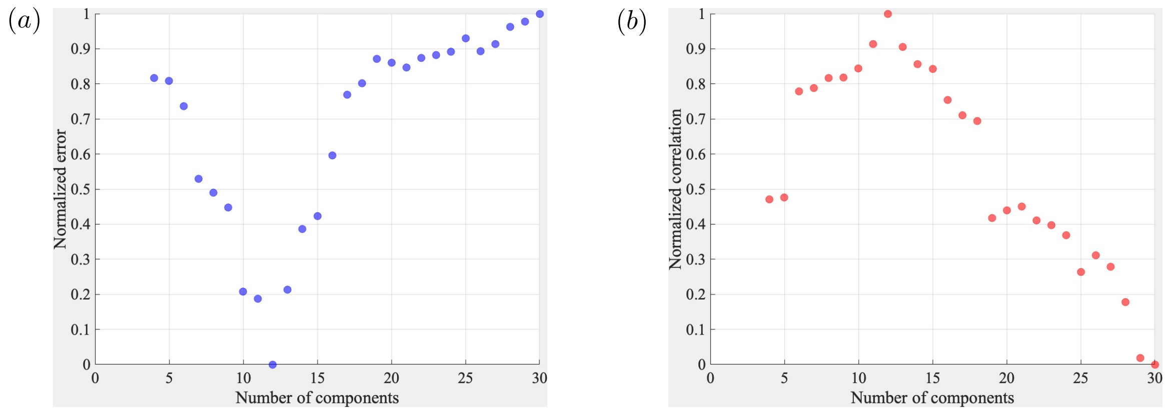

Figure 10: Accuracy of different reconstruction models.

We sincerely appreciate the reviewer's inquiry and demand. It motivates us to conduct additional research into the SVD results. We examined the residual vector's power spectral density in relation to each SVD basis (See Fig. 11). It confirms our belief in high modes. The temporal coefficients of spatial SVD modes, like many SVD/POD-based applications (for example, analyzing flow over a cylinder), typically contain a mix of frequencies. Because we used experimental data, incoherent noise in the data appears as high-order SVD modes. Simply removing high-order modes from the expansion removes the incoherent noise from the dataset. However, it is not always clear how many SVD modes should be retained, and there are numerous truncation criteria to choose from [2-4].

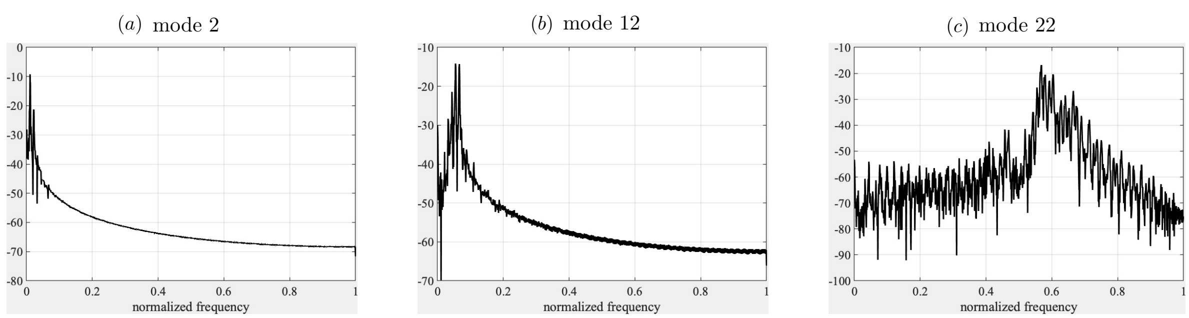

Figure 11: Power spectral density of different eigen-modes.

- 1. Goodfellow, I., Bengio, Y. and Courville, A., 2016. Deep learning. MIT press.
- 2. Epps, B.P. and Krivitzky, E.M., 2019. Singular value decomposition of noisy data: noise filtering. Experiments in Fluids, 60(8), pp.1-23.
- 3. Nekkanti, A. and Schmidt, O.T., 2021. Frequency–time analysis, low-rank reconstruction and denoising of turbulent flows using SPOD. Journal of Fluid Mechanics, 926.
- 4. Epps, B.P. and Krivitzky, E.M., 2019. Singular value decomposition of noisy data: mode corruption. Experiments in Fluids, 60(8), pp.1-30.

To Comment #11

Concern: ***Please explain the smaller predicted amplitude for the training set and test set in Figure 12? The linear frequency seems perfectly captured, could we conclude the ML-based method is more effective for system identification but less useful for time-domain analysis?***

Response: Thank you for your question. (1) In the sparse learning step, we made a rank-r truncation of the Hankel matrix created by delay embedding coordinates. There is an information loss analog to lossy compression; (2) the proposed method focuses on finding a linear representation of nonlinear dynamics. The dynamics are assumed to be linearly propagable using the identified operator matrix. The sloshing dynamics, on the other hand, are not limited to the linear regime. The nonlinear dynamics can be defined as the difference between the truth and the predictions; and (3) The true dynamics are estimated by the SVD algorithm, whose goal is to optimally evaluate the Hankel matrix in an L_2 norm sense. The goal of the regression task is to accurately propagate the dynamics with a set of truncated SVD components. It is reasonable that the regression task might filter out intensify temporal behaviors in order to stably propagate the dynamics.

Because the work presented in this paper is similar to the eigensystem realization algorithm (ERA) [1] and the singular spectrum analysis (SSA) [2], which are both based on the construction of a Hankel matrix from a time series of measurement data, it is reasonable to expect that the proposed algorithm will perform well in system identification tasks. With proper reformulation, for example, adding some equation-based constraints if available and applying the machine learning algorithm to state-space variables to identify Koopman invariant subspaces, the current framework's performance in time-domain analysis tasks could be improved.

- 1. Juang, J.N. and Pappa, R.S., 1985. An eigensystem realization algorithm for modal parameter identification and model reduction. Journal of guidance, control, and dynamics, 8(5), pp.620-627.
- 2. Broomhead, D.S. and Jones, R., 1989. Time-series analysis. Proceedings of the Royal Society of London. A. Mathematical and Physical Sciences, 423(1864), pp.103-121.

To Comment #12

Concern: ***Please also show the validation of prediction performance on both training and testing sets for the nonlinear term Vn. The characteristic change due to nonlinearity observed by this method is essential for the nonlinear sloshing analysis.***

Response: Thank you for the question. The proposed ML framework begins with the embedding of the state-space variable. For example, consider a sloshing sequence of size 2100×1. If the embedding dimension is set to 100, the resulting embedded representation is 2000×100 in size. Then SVD is used, and truncation is performed. For instance, suppose the truncation number is 15. This means that we will use the first 14 SVD components to construct a linear model and the remaining component 15 will act as a nonlinear forcing term. To put it another way, the first 14 components serve as a prediction tool, while the last 15 serves as a system identification tool. That is why, when studying prediction performance, we focus on the leading components, such as the first few components ranked by kinetic energy, rather than the last one. We revised our methodology section to make our presentation more clear.

To Comment #13

Concern: ***Please improve the conclusion by emphasizing the advantages brought by the ML-based method in some specific aspects. For example, your wavelet analysis is a good diagram to show the frequency change during excitations, while the traditional method can complete the same task. So what makes the difference is the novelty of the paper.***

Response: We appreciate the reviewer's suggestion. To highlight the unique property of machine learning-based methods, we revised our concluding part accordingly. In addition, we created a figure that highlights the unique perspective of analyzing data from traditional wavelets and the proposed machine learning method. This is also included in the supplemental material we created, which is available at `https://github.com/Xihaier/ML_Sloshing_Characterization`.

Revised Conclusion

This paper proposes a framework for characterizing the dynamics of nonlinear and non-Gaussian liquid sloshing. In comparison to traditional system identification methods like wavelet, the proposed machine learning framework provides approximate linear representations of nonlinear dynamics. To address the data rank-deficiency, spectral decomposition is applied to time delay coordinates given a sequence of wave elevation. Then, using a set of decomposed eigenvectors, sequential sparse regression is utilized to identify an intermittently forced linear system. As a result, when compared to traditional approaches, the model's transparent data-driven structure and fast machine learning computation make it an excellent candidate for online feedback control tasks. In future work, it is worthwhile to incorporate well-established controlling strategies into the current framework.

Through the use of a wide range of experimental data, we demonstrated the model is capable of accurately representing embedded sloshing sequences. Meanwhile, a series of statistical tests show

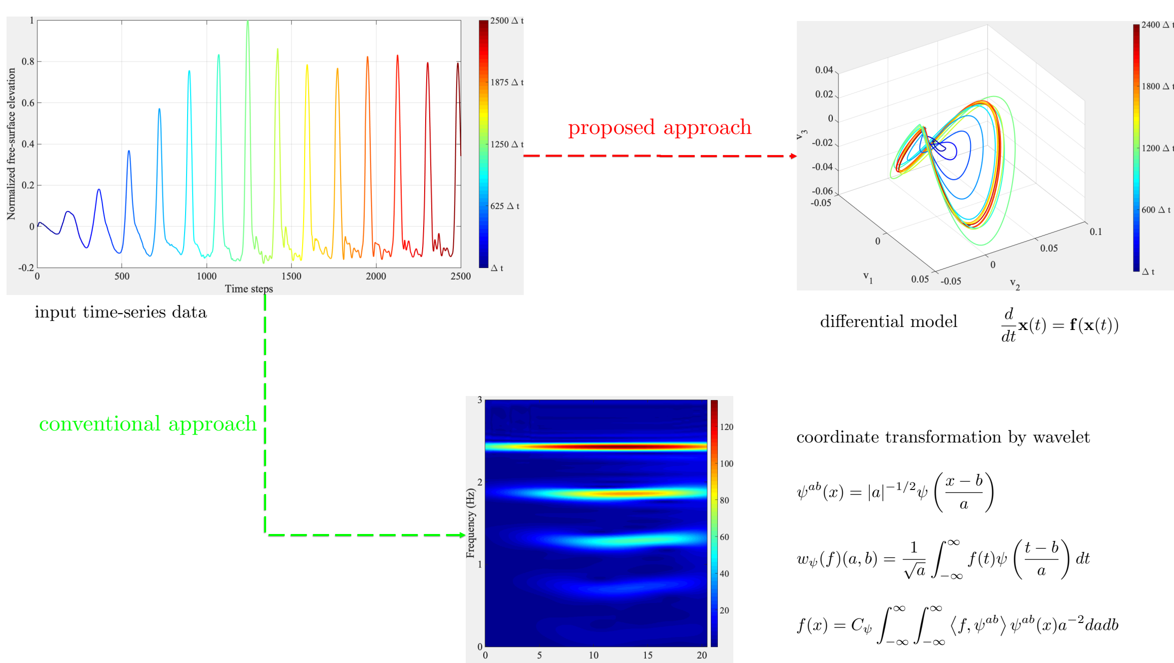

Figure 12: Comparison between traditional wavelet and proposed machine learning framework.

that the model captures chaotic behaviors like bursting and switching in the embedded sequence. Various performance metrics are used to demonstrate the accuracy of the multi-step prediction results. Admittedly, liquid sloshing can cause complex nonlinearities such as out-of-plane sloshing, spinning, irregular beat vibration, and pseudo-periodic motions. These nonlinearities are far more complex than the wave elevation dynamics we observed. Extending the methodology described here to different types of moving water waves, using either high fidelity CFD simulation data or more delicate experiment measurements, is a desirable first step toward developing a more robust and general data-driven simulation strategy for sloshing dynamics.

To Comment #14

Concern: ***Please enlarge Figures 7, 9, 10, and 11 for clear review.***

Response: Having such a responsible and accountable reviewer during the pandemic is truly a blessing. The panel size of the listed figures has been altered. If we are accepted, we will also work with the publisher to ensure that high-quality figures are included in the final publication.

To Comment #15

Concern: ***Please add units in the horizontal and vertical axes for figures.***

Response: Yes, we double-check our figures to ensure that the correct units are included. It is worth noting that because we use eigenvectors as a baisis, we do not provide units to the attractor-associated results. In practice, it is usually best to make them dimensionless so that their norms are all the same.

To Comment #16

Concern: ***Did you record the experimental sloshing pressure or force? Sometimes the nonlinearity and fast momentum change can be observed via force more easily.***

Response: Yes, we agree with the reviewer that detecting pressure or force can be more effective in studying nonlinear sloshing dynamics in some cases. Such aspects are not covered by the experiments described in this paper. In the future, we may consider installing new types of sensors to better monitor the nonlinear dynamics.

Second Round Discussion

- Participant
  - Atilla Incecik
  - Reviewer #1
  - Xihaier Luo
  - Ahsan Kareem
  - Liting Yu
  - Shinjae Yoo
- Time: March, 17, 2022 - April, 9, 2022

To Editor-In-Chief:

Dear Prof. Atilla Incecik,

We are writing below following the receipt of comments regarding our paper, *A Machine Learning-based Characterization Framework for Parametric Representation of Nonlinear Sloshing*. The summary via system notification stated that the paper may need a little bit further revision. We are writing to seek your assistance to better understand and address the reviewer's comments or an editorial decision from your end as the Editor-in-Chief.

Reviewer Comments

The revision decision comments are as follows:

- Reviewer #1: Although the author has made necessary revision to the manuscript, there are still some important suggestions that need to be considered before it can be accepted for publication.
  1. As for the reviewer's comments 3, the author's answer is not satisfactory to the reviewer.
  2. All diagrams except figures 1 to 3 need to be redrawn, which are not clear enough and too rough in the current version.
  3. The paper is too long for readers to read, please cut it down to 20 pages or less.
- Reviewer #3: The authors addressed the comments properly and so the manuscript may be accepted.

Author Responses

We think that the first reviewer may have difficulty accessing the figures:

1. In the last round, he/she mentioned that Fig.6 was missing from the manuscript. That was not the case as the file history would suggest. Also, the other reviewers in the group noted full access to all figures.
2. In this round, the reviewer asks to regenerate all figures because the current version isn't clear enough and is too rough. Could there be a problem with transferring our article to the reviewer via the web system because all of our figures are indeed in a high resolution? If you could kindly spare a few moments, please review our paper and zoom in on the figures. We are sure you would agree with us. On the other hand, the other reviewer previously commented on the figure's units, indicating he/she has no problem reading our figure, even examining the units. Based on these, there appears to be some communication issue that may frustrate the first reviewer.

Secondly, Rev #1 commented that the paper is too long for readers to read, please cut it down to 20 pages or less. We are a bit puzzled by this suggestion as it was not in the first review. In addition, in the last round, the reviewer asked to cite two papers from the same group and add comments on their work. We were also asked to provide more detailed information about our experiments. We complied with these suggestions which led to adding additional length. If the reviewer is referring to the publication style, the manuscript is formatted in [final,3p, times] within 20 pages. Furthermore, we believe that domain-leading journals, such as Ocean Engineering, focus on the research work rather than the format style, and that publication staff can further ensure that good work is presented in the best way possible to meet the requirements.

Finally, the last issue is with the reviewer's comments 3, the author's answer is not satisfactory to the reviewer. The original comment #3 was In section 3.4, *it is difficult to distinguish chaotic motion of free surface from the trajectories plotted in the reconstructed phase space. In fact, according to the external excitation frequency and the geometry of the cavity, the liquid free surface may produce very complex nonlinearities such as out-of-plane sloshing, spinning, irregular beat vibration, pseudo-periodic motion and chaos, these nonlinearities are much more complex than the "elevation first runs up and then runs down" that the authors point out.*

We first and foremost concur with the reviewer's observations regarding the complexities of nonlinear properties of water sloshing, which has been the subject of many papers and books. Each contribution can address a part of the whole problem and with cumulative effort one may reach the point that can address the philosophical concern the reviewer expressed. We never claimed that our contribution will be the conclusive and comprehensive answer to the challenges. If it models – elevation first runs up and then runs down—is a good beginning. It's very rare to see such general comments lacking a definitive point without any guidance on what exactly is broke. We informed all of the reviewers that we plan to upgrade our experiment equipment and conduct CFD simulations in the future to further investigate this long-standing challenging problem (We even shared some of our preliminary CFD simulation results). As you may be very aware, conducting a reliable and systematically validated CFD model for such a complex problem can take months or even years of effort, let alone implementing a new set of test platforms. As a result, we are unsure how to properly respond to the reviewer's comment at this time.

Given the amount of effort in the original submission and review cycle and then a second round after we complied with the comments (**20 pages of detailed response**) to the best of our ability, we suspect due to shifting goal post there may be a conflict of interest. Accordingly, we would request that as the Editor-in-Chief you may consider evaluating our 20-page response to the first round and in this message and make a decision accordingly on our submission.

Kind regards,

Third Round Discussion

- Participant
  - Atilla Incecik
  - Reviewer #1
  - Xihaier Luo
  - Ahsan Kareem
  - Liting Yu
  - Shinjae Yoo
- Time: April, 9, 2022 - present

To Reviewer #1

To The Second-Round Comments:

Concern: ***Although the author has made necessary revision to the manuscript, there are still some important suggestions to which the author didn't give considerable concern. Based on the above reasons, the reviewer has to recommend the revised manuscript be rejected for publication. The reviewer now carefully remind that, in the previous round, the comment 3 is shown as follows: In section 3.4, it is difficult to distinguish chaotic motion of free surface from the trajectories plotted in the reconstructed phase space. In fact, according to the external excitation frequency and the geometry of the cavity, the liquid free surface may produce very complex nonlinearities such as out-of-plane sloshing, spinning, irregular beat vibration, pseudo-periodic motion and chaos, these nonlinearities are much more complex than the "elevation first runs up and then runs down" that the authors point out. The paradox is, the author misunderstand reviewer's suggestion. Also, it is regret, beside other problems (for example, the quality of figures in new version is still not up to publication standards), the more serious problem is found in the revised version. It is detailed as follows. In Section 4, the author wrote "......learning framework provides approximate linear representations of nonlinear dynamics." in page 27 (This statement is in Section 3 of the previous version—the author has clipped him to the conclusion in Section 4). The reviewer absolutely disagrees with the author because that nonlinear properties cannot be reflected by linear system. This fully shows that the author's understanding of the nature of nonlinearity is not deep enough. In addition, if the paper is accepted for publication, the author's views will also mislead readers.***

Response Summary: We appreciate the reviewer's additional comments on the paper. There appears to be some misunderstanding based on the thread of our discussion. The reviewer's main concern now appears to be the linear representation of the nonlinear dynamics and a challenge to the depth of our understanding. Accordingly, we have revised and improved the methodology section of our manuscript on representation learning and its connection to cutting-edge nonlinear dynamics analysis theories and algorithms such as the Koopman operator, dynamic mode decomposition, and others. A detailed discussion of learning the linear representation of nonlinear dynamics is also provided here to assist the reviewer in better understanding the method we proposed and avoiding unnecessary misunderstanding.

Detailed Response:

Problem Setup

First and foremost, we would like to provide a preliminary definition of the dynamical system under consideration in this paper. Consider a general vector field $\mathcal{S}$, latent variable $\boldsymbol{u}$ is evolving in this vector field. Because of limited facilities and costly instrumentation, one is frequently limited to a small number of measurements $\boldsymbol{x}$:

$$\boldsymbol{x} = f \circ \boldsymbol{u} \tag{4}$$

where $\circ$ denotes the composition operator and f is the observation function. In the context of sloshing, $\boldsymbol{u}$ can be the pressure or free-surface displacement field and f is the sensor used to track the wave elevation. Consequently, $\boldsymbol{u} \in \mathcal{S}$ with $\dim(\mathcal{S}) = n$ is observed in a lower rank manifold $\mathcal{A}$ with $\dim(\mathcal{A}) = 1$. To study the dynamical evolution held by $\Phi : \boldsymbol{u}_t \to \boldsymbol{u}_{t+1}$, the low-dimensional observation $\boldsymbol{x}$ is usually projected in a higher rank manifold $\mathcal{B}$ with $\dim(\mathcal{B}) = d$:

$$\boldsymbol{\chi} = p \circ \boldsymbol{x} \tag{5}$$

with p denoting the projection, namely, the embedding function. Through Eq. 5, one can hereafter obtain a topologically equivalent representation $\hat{\Phi} : \boldsymbol{\chi}_t \to \boldsymbol{\chi}_{t+1}$ of the original dynamical map Φ. And latent variable $\boldsymbol{u}$ and embedded variable $\boldsymbol{\chi}$ are intrinsically connected by means of the delay-coordinate map that takes the expression of:

$$D_{(f,\Phi)}(\boldsymbol{u}) : \boldsymbol{u} \mapsto \left[f \circ \boldsymbol{u}, f \circ \Phi(\boldsymbol{u}), \ldots, f \circ \Phi^{d-1}(\boldsymbol{u})\right]^T \tag{6}$$

The delay-coordinate map $D_{(f,\Phi)}(\boldsymbol{u})$ is conditionally deemed to be a delay embedding when the embedding dimension number $d \in \mathbb{R}^+$ satisfies two box-counting constraints: $2\overline{\dim}_B(\mathcal{S}) < d$ and $2\overline{\dim}_B\left(\{\boldsymbol{u} \in \mathcal{S}\} : \Phi^k \boldsymbol{u} = \boldsymbol{u}\right) < \boldsymbol{u}$ for every $k = 1, \ldots, n-1$. Fig. 9 gives a graphic illustration of the aforementioned commutative operations $\boldsymbol{u} \mapsto x \mapsto \boldsymbol{\chi}$.

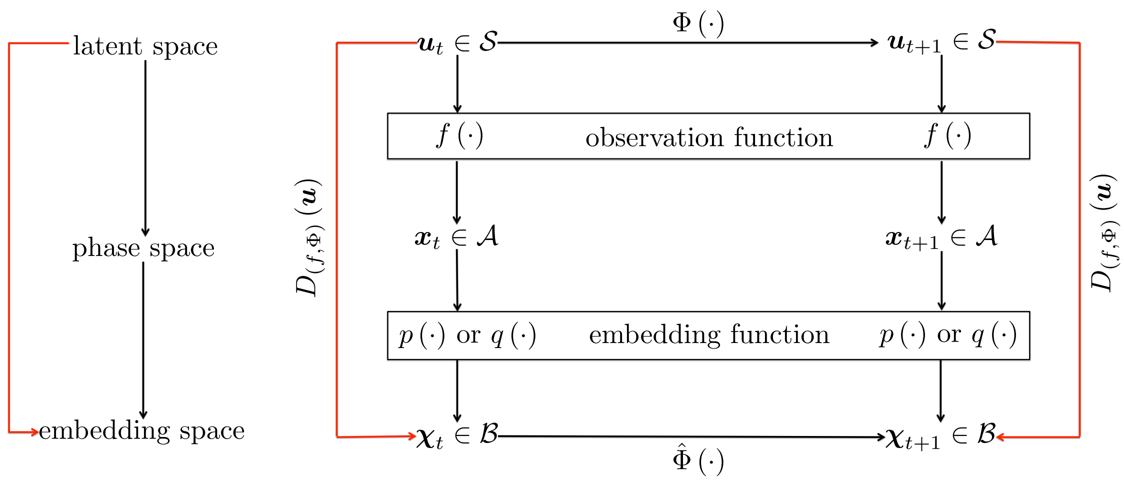

Figure 13: Schematic illustration of nonlinear sequence embedding.

In light of this, the starting point for our analysis is phase space. The reviewer may have misidentified the latent space as the initial, leading to the misunderstanding. We thank the reviewer for drawing our attention to it, and we have highlighted the distinction between phase space and latent space in the manuscript to assist future readers.

Perspectives On Nonlinear Dynamics

Now, the remaining question is whether we can find a faithful linear approximation of the nonlinear dynamics observed in phase space. In order to answer this question, we must return to the leading perspective on nonlinear dynamical systems, which considers the geometry of subspaces of local linearizations around fixed points and periodic orbits, global heteroclinic and homoclinic orbits connecting these structures, and more general attractors. This geometric theory, which originated with Poincaré, has transformed how we model complex systems, and its success can be attributed in large part to theoretical results such as the Hartman-Grobman theorem, which establishes when and where a nonlinear system can be approximated with linear dynamics. As a result, it is frequently practical to apply a plethora of linear analysis techniques in a limited vicinity of a fixed point or periodic orbit. Although the geometric approach gives quantitative locally linear models, global analysis has remained essentially qualitative and computational, confining nonlinear prediction, estimation, and control theory to fixed points and periodic orbits.

The reviewer may have misunderstood our method and thought it belonged to this category. We recognize that such misunderstandings can occur, and we would like to underline that our method is not based on local linear approximation, but rather on operator-theoretic approaches. As we will demonstrate, nonlinear dynamical systems can be represented in terms of infinite-dimensional but linear operators, such as the Koopman operator that advances measurement functions, or the Perron-Frobenius operator, which advances probability densities and ensembles through the dynamics.

Koopman Theory

Consider a nonlinear dynamical system of the form

$$\frac{d}{dt}\mathbf{x}(t) = \mathbf{f}(\mathbf{x}(t)) \tag{7}$$

in the aforementioned phase space on $\mathbb{R}^n$, where $\mathbf{x}$ denotes the system's state, $\mathbf{f}: \mathbb{R}^n \to \mathbb{R}^n$ is a nonlinear vector field, and t denotes time. For fluid dynamics applications such as liquid sloshing, it is common to assume that $\mathbf{f}$ is at least continuous, implying that the trajectories $\mathbf{x}(t)$ are at least $\mathcal{C}^1$. Eq. 7 induces a flow map $\mathbf{F}_t$, specifically a time-dependent family of maps $\{\mathbf{F}_t\}_{t\in\mathbb{R}_+}$, satisfying

$$\mathbf{x}(t) = \mathbf{F}_t(\mathbf{x}_0) \tag{8}$$

which yields the state $\mathbf{x}(t)$ at time t given an initial state $\mathbf{x}_0 := \mathbf{x}(0)$. To address the issue of nonlinearity, B. O. Koopman and J. v. Neumann pioneered an influential operator-theoretic perspective on the above-mentioned dynamical systems. Their fundamental insight was that by considering an appropriately chosen Hilbert space of scalar observable functions $g: \mathbb{R}^n \to \mathbb{C}$ on the state rather than the state directly, the finite-dimensional nonlinear dynamics of Eq. 7 can be transformed to an infinite-dimensional, linear dynamical system. The one-parameter semigroup of Koopman Operators, $\{\mathcal{K}_t\}_{t\in\mathbb{R}_+}$, acting on observables g is defined by

$$\mathcal{K}_t g = g \circ \mathbf{F}_t \tag{9}$$

with $\circ$ representing the composition operator. Combining Eq. 8 and Eq. 9 we have

$$\mathcal{K}_t g(\mathbf{x}_0) = g(\mathbf{F}_t(\mathbf{x}_0)) = g(\mathbf{x}(t)) \tag{10}$$

$\mathcal{K}_t$ is a function that maps the measurement function g to the values it will take after the dynamics have progressed for a time t. The generator of the Koopman operator family is defined as

$$\mathcal{K}g = \frac{d}{dt} g \circ \mathbf{F}_t = \lim_{t\to 0^+} \frac{1}{t}(\mathcal{K}_t g - g) \tag{11}$$

When $\mathbf{F}$ is smooth and globally Lipshitz, the second equality holds in an L_2 sense. Consider a reduced compact domain for a system that is not globally Lipshitz; for L_2 functions with compact support on this domain Ω, the second equation holds in an L_2 sense, even if the dynamics are not globally Lipshitz. In general, for a continuous observable function, this limit holds pointwise rather than in the L_2 sense.

This so-called Koopman operator is linear, and its spectral decomposition fully characterizes the behavior of a nonlinear system. It is, however, infinite-dimensional because there are an infinite number of degrees of freedom required to describe the space of all possible measurement functions g of the state. Our proposed decomposition method, as discussed in the introduction and methodology sections of the paper, seeks to provide finite-dimensional, matrix approximations of the Koopman operator based on spectral decomposition $\mathcal{K}_t \mathbf{g} = \sum_{j=0}^{\infty} \mathbf{c}_j \phi_j(\mathbf{x}_0) e^{2\pi i \omega_j t} + \int dE(\omega) e^{2\pi i \omega}$, where $dE(\omega)$ is the spectral measure associated with the continuous component of the spectrum of $\mathcal{K}_t$. For more detailed proof and deduction, we recommend checking the following references.

1. Koopman, B.O., 1931. Hamiltonian systems and transformation in Hilbert space. Proceedings of the national academy of sciences of the united states of america, 17(5), p.315.

2. Koopman, B.O. and Neumann, J.V., 1932. Dynamical systems of continuous spectra. Proceedings of the National Academy of Sciences, 18(3), pp.255-263.

3. Mezić, I., 2005. Spectral properties of dynamical systems, model reduction and decompositions. Nonlinear Dynamics, 41(1), pp.309-325.

4. Budišić, M., Mohr, R. and Mezić, I., 2012. Applied koopmanism. Chaos: An Interdisciplinary Journal of Nonlinear Science, 22(4), p.047510.

Dynamic Mode Decomposition

We would like to move on to practical implementation now that we've established the theoretical foundation. Dynamic mode decomposition is a leading algorithm that has been developed to aid in the study of the Koopman operator and its spectral properties. Schmid first proposed it to the fluid dynamics community as a tool for extracting spatiotemporal coherent structures from complex flows. The DMD algorithm works exactly as follows:

$$\mathbf{X}_1 = \begin{pmatrix} | & | & & | \\ \mathbf{x}_1 & \mathbf{x}_2 & \cdots & \mathbf{x}_{M-1} \\ | & | & & | \end{pmatrix} \quad \mathbf{X}_2 = \begin{pmatrix} | & | & & | \\ \mathbf{x}_2 & \mathbf{x}_3 & \cdots & \mathbf{x}_M \\ | & | & & | \end{pmatrix} \tag{12}$$

where $\mathbf{X}_1$ and $\mathbf{X}_2$ are two snapshot matrices of state measurements. The algorithm calculates the linear relationship between the data matrices. $\mathbf{x}_j = \mathbf{x}(t_j)$ denotes the j^{th} timestep at discrete time t_j and $\Delta t = t_{j+1} - t_j$. is the timestep between snapshots. The algorithm estimates the propagator matrix that satisfies

$$\mathbf{X}_2 \approx \mathbf{K}\mathbf{X}_1 \tag{13}$$

The optimal $\mathbf{K}$ is found by solving the optimization problem

$$\mathbf{K} = \arg\min_{\hat{\mathbf{K}}} \left\| \hat{\mathbf{K}}\mathbf{X}_1 - \mathbf{X}_2 \right\|_F \tag{14}$$

where $\|\cdot\|_F$ denotes the Frobenius norm defined as $\|\mathbf{X}\|_F = \sqrt{\sum_{j=1}^{n} \sum_{k=1}^{M} X_{jk}^2}$.

These are the basic components of our proposed sequential coefficient optimization algorithm, which is discussed in Section 2.4 (Eq. (5) - Eq. (11)). One thing to keep in mind, as we emphasize in our manuscript and here, is that we use delay embedding to deal with partial state information. This method adds past history to a state represented by a single (or few) measurement function, resulting in a new observable $\tilde{\mathbf{g}}(\mathbf{x}(t)) =: (g(\mathbf{x}(t)), g(\mathbf{x}(t-\Delta t)), g(\mathbf{x}(t-2\Delta t)), \cdots, g(\mathbf{x}(t-n\Delta t)), \cdots, g(\mathbf{x}(t-$

$(N-1)\Delta t))) \in \mathbb{R}^N$ in the embedding space (See Fig. 13). Meaning Eq. (5) in our manuscript can be written using the action of the Koopman operator on g as

$$\mathbf{H} = \begin{pmatrix} g(\mathbf{x}_1) & \mathcal{K}_{\Delta t} g(\mathbf{x}_1) & \cdots & \mathcal{K}_{\Delta t}^{M-1} g(\mathbf{x}_1) \\ \mathcal{K}_{\Delta t} g(\mathbf{x}_1) & \mathcal{K}_{\Delta t}^{2} g(\mathbf{x}_1) & \cdots & \mathcal{K}_{\Delta t}^{M} g(\mathbf{x}_1) \\ \vdots & \vdots & \ddots & \vdots \\ \mathcal{K}_{\Delta t}^{N-1} g(\mathbf{x}_1) & \mathcal{K}_{\Delta t}^{N} g(\mathbf{x}_1) & \cdots & \mathcal{K}_{\Delta t}^{M+N-2} g(\mathbf{x}_1) \end{pmatrix} = \begin{pmatrix} | & | & & | \\ \tilde{\mathbf{g}}(\mathbf{x}_1) & \mathcal{K}_{\Delta t} \tilde{\mathbf{g}}(\mathbf{x}_1) & \cdots & \mathcal{K}_{\Delta t}^{M-1} \tilde{\mathbf{g}}(\mathbf{x}_1) \\ | & | & & | \end{pmatrix} \tag{15}$$

As indicated in the revised manuscript, Eq. (6) in our manuscript is performed using this Hankel representation of the data. We recommend reading the following references for more information on dynamic mode decomposition.

1. Schmid, P.J., 2010. Dynamic mode decomposition of numerical and experimental data. Journal of fluid mechanics, 656, pp.5-28.

2. Lan, Y. and Mezić, I., 2013. Linearization in the large of nonlinear systems and Koopman operator spectrum. Physica D: Nonlinear Phenomena, 242(1), pp.42-53.

3. Jovanović, M.R., Schmid, P.J. and Nichols, J.W., 2014. Sparsity-promoting dynamic mode decomposition. Physics of Fluids, 26(2), p.024103.

4. Pan, S. and Duraisamy, K., 2020. On the structure of time-delay embedding in linear models of non-linear dynamical systems. Chaos: An Interdisciplinary Journal of Nonlinear Science, 30(7), p.073135.

With this additional discussion, we sincerely hope that the previous misunderstanding about linear representation learning in nonlinear dynamics has been clarified and that the reviewer has better understanding of our presentation.

Decision

- Initial decision
  - reviewer 1
  - Reviewer #1: This paper presents a data-driven framework for modeling nonlinear sloshing dynamics. The proposed scheme is based on gradient-based embedding, spectral decomposition, and sequential sparse regression. The average mutual information and false nearest neighbors method were considered to select the delay step and embedding dimension in phase space reconstruction. The embedded sloshing sequence is subsequently decomposed into two parts: linear evolution and nonlinear excitation. A predictive model is developed using the decomposed components. The method proposed is innovative and the scientific quality of this manuscript is generally satisfactory. In this sense, this manuscript brings substantial new contributions. Based on that, I do recommend the acceptance of this manuscript after the following aspects are improved.
  - Reviewer #3: This paper analyzes the sloshing phenomenon in the ML-based framework. The advantage of ML is that simulation can be reproduced without utilizing any governing equations. This paper has shown the potential of the ML-based method for solving the sloshing problem. The authors demonstrated their numerical methods for characterizing the sloshing phenomenon in a tank with slat screens. The topic is of interest and the problem is worthy of study. The paper is well written. The following comments should be addressed before the recommendation of the paper for publication in "Ocean Engineering".

- Final comments from the Reviewer #1
  - The reviewer absolutely disagreed with the authors' opinion that "...... provides approximate linear representations of nonlinear dynamics.....", this unscientific statement should not appear in a high-level academic journal like Ocean Engineering.
  - In section 3.3, the author wrote " In the beginning, the attractor chaotically oscillates in space ". From the point of view of nonlinear dynamics, this statement has no academic significance.
  - Figure 9 was not found in the manuscript.
  - In figure 13, the power spectral density are all presented with negative value, is it reasonable?
  - In section 3.4, the author wrote "Meanwhile, as illustrated in Fig. 11. (a), the initial states are more chaotic and less constrained by the embedded attractor." In fact, there is nothing to do with the chaos as we can see from Fig. 11. (a). It is very regrettable that the author exaggerates his work in such an irresponsible manner.
  - The labels in Figures 4 and 10 are too small to see clearly—-this problem has been pointed out previously, but the author refused to improve the figures' quality. The reviewer believe that the author's work is both rough and sloppy.

- Final decision
  - Thank you very much for revising your paper. I am very sorry to inform you that based on the reviewer's comments I am unable to accept your paper for publication in Ocean Engineering.
- Invitation

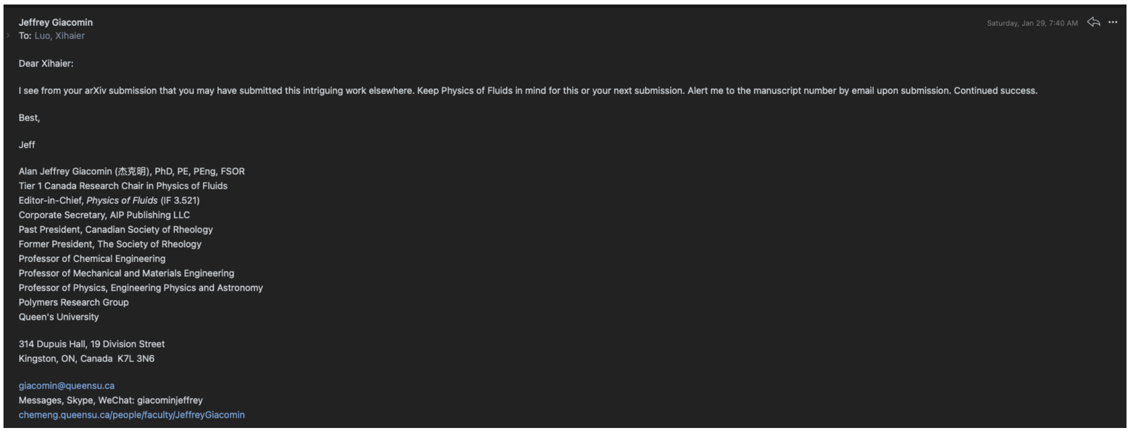

Jeffrey Giacomin
Saturday, Jan 29, 7:40 AM
To: Luo, Xihaier

Dear Xihaier:

I see from your arXiv submission that you may have submitted this intriguing work elsewhere. Keep Physics of Fluids in mind for this or your next submission. Alert me to the manuscript number by email upon submission. Continued success.

Best,

Jeff

Alan Jeffrey Giacomin (杰克明), PhD, PE, PEng, FSOR
Tier 1 Canada Research Chair in Physics of Fluids
Editor-in-Chief, *Physics of Fluids* (IF 3.521)
Corporate Secretary, AIP Publishing LLC
Past President, Canadian Society of Rheology
Former President, The Society of Rheology
Professor of Chemical Engineering
Professor of Mechanical and Materials Engineering
Professor of Physics, Engineering Physics and Astronomy
Polymers Research Group
Queen's University

314 Dupuis Hall, 19 Division Street
Kingston, ON, Canada K7L 3N6

giacomin@queensu.ca
Messages, Skype, WeChat: giacominjeffrey
chemeng.queensu.ca/people/faculty/JeffreyGiacomin

References

[1] L. Yu, M.-A. Xue, and J. Zheng, “Experimental study of vertical slat screens effects on reducing shallow water sloshing in a tank under horizontal excitation with a wide frequency range,” *Ocean engineering*, vol. 173, pp. 131–141, 2019.

[2] L. Yu, M.-A. Xue, and Z. Jiang, “Experimental investigation of parametric sloshing in a tank with vertical baffles,” *Ocean Engineering*, vol. 213, p. 107783, 2020.

[3] O. M. Faltinsen, “A nonlinear theory of sloshing in rectangular tanks,” *Journal of Ship Research*, vol. 18, no. 04, pp. 224–241, 1974.

[4] B. Molin and F. Remy, “Experimental and numerical study of the sloshing motion in a rectangular tank with a perforated screen,” *Journal of Fluids and Structures*, vol. 43, pp. 463–480, 2013.

[5] O. M. Faitinsen, “A numerical nonlinear method of sloshing in tanks with two-dimensional flow,” *Journal of Ship Research*, vol. 22, no. 03, pp. 193–202, 1978.

[6] J. Cho, H. Lee, and S. Ha, “Finite element analysis of resonant sloshing response in 2-d baffled tank,” *Journal of Sound and vibration*, vol. 288, no. 4-5, pp. 829–845, 2005.

[7] K. Biswal, S. Bhattacharyya, and P. Sinha, “Non-linear sloshing in partially liquid filled containers with baffles,” *International Journal for Numerical Methods in Engineering*, vol. 68, no. 3, pp. 317–337, 2006.

[8] M.-A. Xue and P. Lin, “Numerical study of ring baffle effects on reducing violent liquid sloshing,” *Computers & Fluids*, vol. 52, pp. 116–129, 2011.

[9] D. Liu and P. Lin, “Three-dimensional liquid sloshing in a tank with baffles,” *Ocean engineering*, vol. 36, no. 2, pp. 202–212, 2009.

[10] D. Liu, W. Tang, J. Wang, H. Xue, and K. Wang, “Comparison of laminar model, rans, les and vles for simulation of liquid sloshing,” *Applied Ocean Research*, vol. 59, pp. 638–649, 2016.

[11] T. Yong and Y. Baozeng, “Simulation of large-amplitude three-dimensional liquid sloshing in spherical tanks,” *AIAA Journal*, vol. 55, no. 6, pp. 2052–2059, 2017.

[12] Y. Tang, B. Yue, and Y. Yan, “Improved method for implementing contact angle condition in simulation of liquid sloshing under microgravity,” *International Journal for Numerical Methods in Fluids*, vol. 89, no. 4-5, pp. 123–142, 2019.

[13] A. S. Iglesias, L. P. Rojas, and R. Z. Rodríguez, “Simulation of anti-roll tanks and sloshing type problems with smoothed particle hydrodynamics,” *Ocean Engineering*, vol. 31, no. 8-9, pp. 1169–1192, 2004.

[14] M. Liu and G. Liu, “Smoothed particle hydrodynamics (sph): an overview and recent developments,” *Archives of computational methods in engineering*, vol. 17, no. 1, pp. 25–76, 2010.